Fluid Phase Equilibria 271 (2008) 94–102

Contents lists available at ScienceDirect

Fluid Phase Equilibria

journal homepage: www.elsevier.com/locate/fluid

Letter to the Editor

Deriving linear isotherms for solids

ARTICLE INFO

Keywords:
Equation of state
Linear isotherm regularity
Solid state
Average effective pair potential
Non-ideal thermal

ABSTRACT

In this paper, we have derived two equations of state, one for the metallic and ionic solids and the other for the remaining solids on the basis of the concept of the average effective pair potential (AEPP). According to the former EOS, $(Z-1)\upsilon^2$ is linear with respect to $1/\rho$, where Z is the compressibility factor and $\upsilon = 1/\rho$ is the molar volume for each isotherm. On the basis of the latter EOS, $(Z-1)\upsilon^2$ is a linear function in terms of ρ^2 for each isotherm. As these EOSs suggest, the temperature dependencies of the internal energy is separable from its density dependencies. Hence, the heat capacity of a solid is independent of its density, interaction potential parameters and non-ideal thermal pressure. However, unlike the heat capacity, the isothermal compressibility and isobaric thermal expansivity both depend on all of them. The linear parameters of the EOSs are related to the average interaction coefficients at zero temperature and also vibrational energy. Since the temperature dependencies of the parameters of both equations are simple, they may, successfully, be applied to the study of the *pVT* behavior of solids at high temperatures. Using only two parameters which are physically interpretable as well as being able to predict at least two regularities in solids are the merits of the new equations of state. In short, these EOSs can open a new window to investigate the EOSs in solids just like the LIR EOS in fluids.

1. Introduction

The equations of state (EOSs) of solids play an important feature in the condensed matter physics and geophysics. They provide numerous information of non-linear compression of materials at high pressure, and have been widely applied to engineering and other scientific researches. Most of the EOSs depend on the three zero-pressure parameters: the molar volume, v_0, the isothermal bulk modulus, B_0, and its isothermal pressure derivative, B_0'. One of the most successful isothermal EOSs is proposed by Vinet et al. [1] which is valid for all classes of solids in compression and in the absence of phase transition. The basis of this EOS is a universal relation for the binding energy in terms of the intermolecular distance. In derivation of this EOS the thermal pressure is neglected, and the volume derivative of the binding energy is used to approximate the internal energy. Another well-known universal EOS for different solids was presented by Parsafar and Mason [2] only with fitting the rather featureless repulsive branch of the binding energy curve into a cubic equation in terms of density. The final result is that $p\upsilon^2$ is a quadratic in density for each isotherm which its scaling parameters can be related to v_0, B_0 and B_0' in the absence of phase transition.

On the other hand, in a series of works the linear isotherm regularity (LIR) [3] originally devised for normal dense fluids, was applied to all kinds of fluids [4,5] and also dense fluid mixtures [6,7]. The LIR is able to predict many experimentally known regularities for pure dense fluids and fluid mixtures [8–11]. According to the LIR EOS, $(Z-1)\upsilon^2$ is linear with respect to ρ^2 for each isotherm of a fluid for densities greater than the Boyle density and temperatures lower than twice of the Boyle temperature.

In this study, we have extended LIR EOS for solids and investigate its accuracy for different classes of solids including monatomic, diatomic, metallic and ionic solids.

This paper is organized as follows: Section 2 presents how LIR can be extended to the non-ionic and non-metallic solids. We further check the accuracy of the new EOS with the experimental data. Additionally, the temperature dependencies of the parameters of this EOS are examined. In Section 3, we do the same task for the metallic and ionic solids. We will proceed with investigating the temperature and density dependence of some physical properties in Section 4. In Section 5, we compare the new EOSs with some of the most successful EOSs proposed in the literature for solids. In Section 6, two regularities predicted by the new EOSs for solids Xe and Au are investigated. This is followed in the last section by a discussion and conclusion.

2. Deriving linear isotherm for the non-ionic and non-metallic solids

2.1. Theoretical aspects

The LIR EOS was derived on the basis of the exact thermodynamic expression,

$$p = T\left(\frac{\partial p}{\partial T}\right)_{\upsilon} - \left(\frac{\partial E}{\partial \upsilon}\right)_{T} \tag{1}$$

0378-3812/$ – see front matter © 2008 Elsevier B.V. All rights reserved.
doi:10.1016/j.fluid.2008.07.009

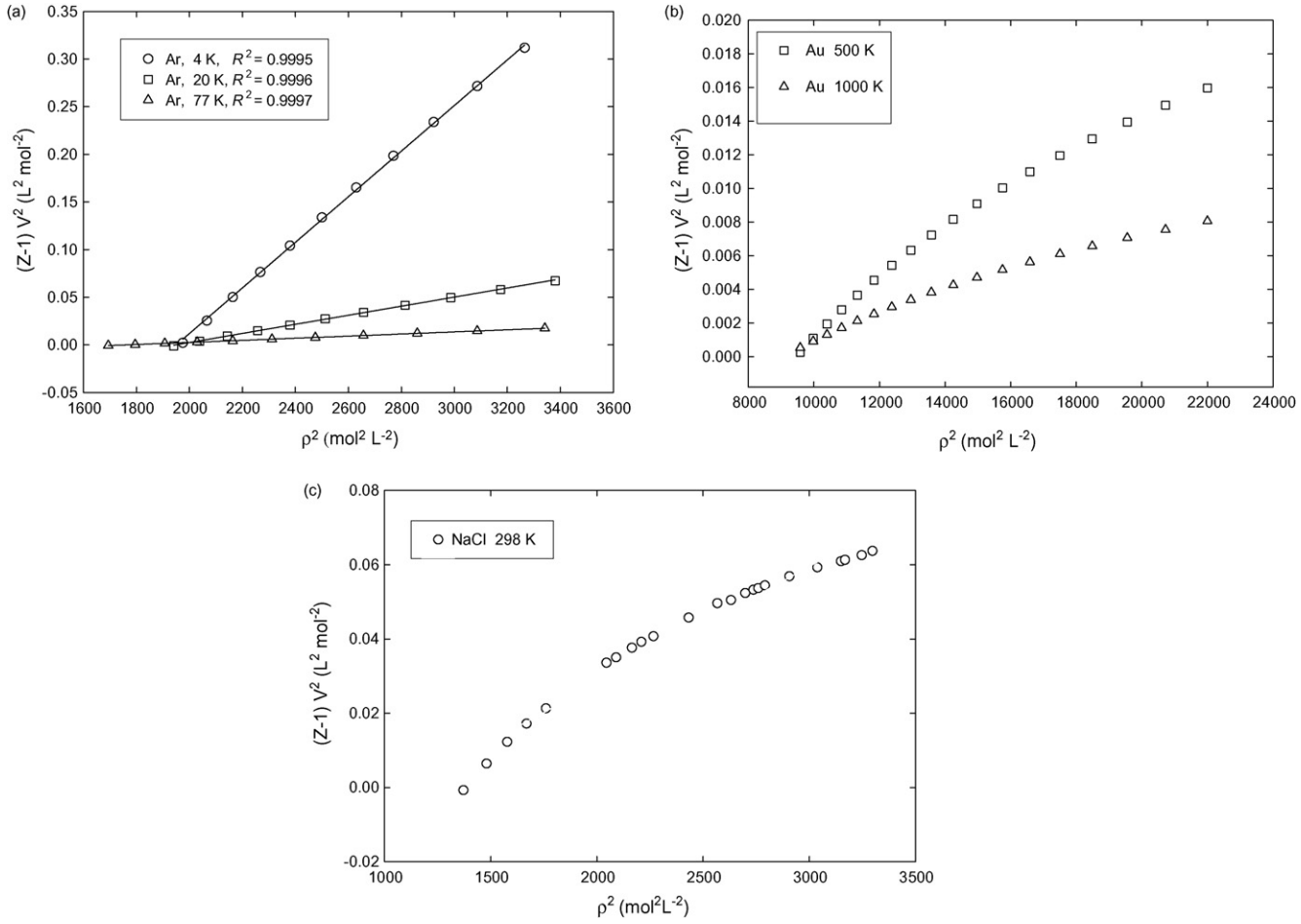

Fig. 1. Fitting experimental data of given isotherm(s) into EOS I for (a) Ar, (b) Au, (c) NaCl. Note the significant nonlinearity of the last two cases.

and also the assumption that the average effective pair potential (AEPP) is a Lennard–Jones (12, 6) function; where p is pressure, T is temperature, and E is internal energy. The AEPP is the average effective pair potential on which the medium effects and the long-range interactions are included. According to Eq. (1), there are two contributions to the pressure; the dominating one for solids is the internal pressure which is related to the binding or static-lattice energy (E_0) and vibrational energy (E_{vib}):

$$E = E_0 + E_{vib} \tag{2}$$

For a large number of fluids and solids, LJ (m–n) potential function has been used for the pairwise interaction approximation between atoms or molecules as the major interaction [12,13]. In the case of many-body systems in which many particles are interacting, this kind of potential is considered to be the interaction of two nearest neighbor molecules in which all of their longer range interactions are added, and also the effect of the medium on the charge distributions of two neighboring molecules is included [14]. Therefore we may write:

$$E_0 = \frac{N}{2} C\varepsilon \left[\left(\frac{\sigma}{r}\right)^m - \left(\frac{\sigma}{r}\right)^n \right] = K_m \rho^{m/3} - K_n \rho^{n/3} \tag{3}$$

where N is the number of particles, C is coordination number which is a constant for a given solid, r is the nearest-neighbor separation, σ and ε are the potential parameters of the AEPP and K_m and K_n are constants whose values depend on the lattice. On the other hand, vibrational energy may be given by the Einstein model, according to which,

$$E_{vib} = 3\,N\,k\,\theta_E \left\{ \frac{1}{2} + \frac{1}{\exp(\theta_E/T) - 1} \right\} \tag{4}$$

where θ_E is the Einstein characteristic temperature and k is the Boltzmann constant.

Although the binding energy has the largest contribution to the internal energy, the vibrational energy term usually determines the stable high-temperature crystal structure and makes a non-negligible contribution to the pressure and energy.

We now consider the Mie–Gruneisen equation which is widely used in the correlation shock-wave experiment as well as in generating the EOS from p–V–T measurements [15]. This equation expresses the pressure as a function of volume and temperature as,

$$p(v, T) = -\left(\frac{\partial E_0}{\partial v}\right) + \frac{\gamma}{v} E_{vib} \tag{5}$$

where γ is known as the Gruneisen parameter. It is worth noting that Eq. (5) may be derived from Eqs. (1) and (4), in which,

$$\left(\frac{\partial p}{\partial T}\right)_v = \frac{\gamma C_V}{v} \tag{6}$$

where C_V is the heat capacity at constant volume. Although here the Einstein model was used for the vibrational energy, one may

Table 1
The parameters of EOS I (a and b), coefficient of determination (R^2), range of pressure data (Δp) and calculated percent density deviation $(\Delta\rho/\rho)\times 100$ for some isotherms of the given solids

Solid	T (K)	$-a$ ($\times 10^2$ L^2 mol^{-2})	b ($\times 10^5$ L^4 mol^{-4})	R^2	Δp (kbar)	100 ($\lvert\Delta\rho\rvert/\rho$)[a]
[b]Ar	4	45.764	23.428	0.9995	0–21	0.13 (0.35)
	20	9.0097	4.6253	0.9996	0–21	0.15 (0.2)
	40	4.2401	2.2312	0.9999	0–21	0.09 (0.24)
	60	2.6315	1.4340	0.9999	0–21	0.05 (0.14)
	77	1.8996	1.0755	0.9997	0–21	0.15 (0.18)
[b]Kr	4	93.020	68.692	0.9996	0–21	0.11 (0.15)
	20	18.449	13.664	0.9999	0–21	0.05 (0.14)
	40	8.7343	6.6085	1.0000	0–21	0.03 (0.10)
	60	5.5202	4.2953	1.0000	0–21	0.01 (0.08)
	77	4.1599	3.3101	0.9999	0–21	0.08 (0.14)
	90	3.4039	2.7681	0.9998	0–21	0.11 (0.29)
	100	2.9510	2.4474	0.9997	0–21	0.16 (0.43)
	110	2.5816	2.1852	0.9996	0–21	0.19 (0.49)
[b]Xe	4	216.49	262.37	0.9998	0–21	0.08 (0.25)
	20	42.556	51.761	0.9997	0–21	0.09 (0.28)
	40	20.764	25.588	0.9998	0–21	0.07 (0.18)
	60	13.271	16.685	0.9999	0–21	0.07 (0.18)
	80	9.7133	12.438	1.0000	0–21	0.01 (0.02)
	100	7.4038	9.7059	1.0000	0–21	0.01 (0.03)
	120	5.9258	7.9357	1.0000	0–21	0.01 (0.04)
	140	4.8577	6.6597	0.9999	0–21	0.06 (0.16)
	159	4.0142	5.6660	0.9997	0–21	0.12 (0.40)
[c]n-H_2	4.2	3.1121	1.6885	0.9992	0–25	0.49 (2.56)
[c]n-D_2	4.2	3.7321	1.5045	0.9995	0–25	0.33 (1.23)
[d]Ne	4	4.2567	0.83045	0.9980	0–20	0.32 (0.97)
[d]N_2	65	2.5728	2.1851	0.9985	0–10.2	0.36 (1.19)
[e]Polyethylene	329	1.9899	1.6024	0.9996	0.001–2	0.025 (0.04)

[a] The maximum percent deviation is given in the parentheses.
[b] Ref. [18].
[c] Ref. [20].
[d] Ref. [19].
[e] Ref. [21].

obtain Eq. (5) for a harmonic solid regardless of the model used for the vibrational energy [16].

As in a dense fluid with spherical molecules, in which each molecule is surrounded with its nearest neighbor symmetrically, it is reasonable to assume that the AEPP is given by an LJ (12, 6) function for a molecular solid. Substituting the LJ (12–6) potential function as the binding energy in Eq. (3) and making use of Eq. (5), the final form of the EOS may be obtained as (hereafter referred to as EOS I),

$$(Z-1)\upsilon^2 = a + b\rho^2 \tag{7}$$

where Z is the compressibility factor, $\rho = 1/\upsilon$ is the molar density and a and b are temperature-dependent parameters, as follows:

$$a = a_2 + \frac{a_1}{T} \tag{8a}$$

and

$$b = \frac{b_1}{T} \tag{8b}$$

where a_1 and b_1 are related to the attraction and repulsion terms of the average effective pair potential, respectively, while a_2 is equal to,

$$a_2 = \frac{1}{\rho^2}\left[\frac{1}{\rho RT}\left(\frac{\gamma}{\nu}E_{\text{vib}}\right) - 1\right] \tag{9}$$

However, one may find different powers for ρ and ν in Eq. (7) for dense fluids. As explained in Ref. [3], the average molecular separation in a dense fluid is around the minimum of the interaction potential function, which is a U-shape curve. Unlike the whole range of interaction potential function (hence entire density range), the U-shape curve may be adequately expressed by a Lennard–Jones (m, n) function with different values for the (m, n) pair.

According to Eq. (9), a_2 seems to be a complicated function in terms of T and ρ. However, its corresponding expression known as the non-ideal thermal pressure was found to be almost a small constant for dense fluids [3,17]. Since the contribution of the thermal pressure in solids is expected to be smaller than that of fluids at the same temperature, one may expect that a_2 is a constant. Such an expectation will be checked by using experimental pVT data of solids, later.

2.2. Experimental test of EOS I for non-ionic and non-metallic solids

To examine the accuracy of the derived EOS I, we serve Ar, Au and NaCl as atomic, metallic and ionic solids, respectively. Fig. 1a shows that the experimental data [18] of Ar are well fitted into EOS I. However, Fig. 1b and c shows that EOS I is not suitable neither for Au nor for NaCl.

Observing the above results, some monatomic and diatomic solids such as neon, argon, krypton, xenon, n-H_2, n-D_2, nitrogen and one semi-crystalline polymer are used as our experimental test of solids. The results of fitting experimental data of the rare gases solids including argon [18], krypton [18], xenon [18] and neon [19] and n-H_2 [20], n-D_2 [20], nitrogen [19], and one semi-crystalline polymer [21] into EOS I are summarized in Table 1 for which the scaled parameters, pressure range of experimental data, coefficient of determination (R^2), and the average percent

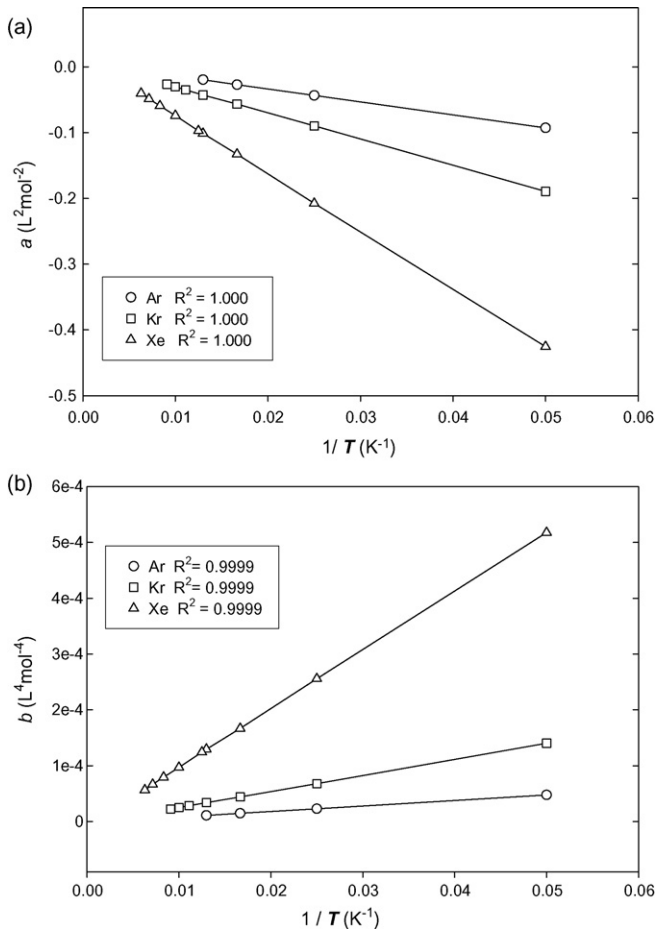

Fig. 2. Temperature dependence of (a) the intercept a and (b) slope b parameters, for Ar, Kr and Xe which all are well fitted into Eqs. (8a) and (8b).

deviation of the calculated density are given for some given isotherms.

2.3. Temperature dependencies of the parameters of EOS I

Having the temperature dependence of the parameters of an EOS, can, in turn, increase the power of our prediction from minimum input data. This is particularly important in geophysical applications, for instance, where knowledge of high pressure is often considered necessary.

In Section 2.1, we presented a model for the temperature dependencies of the scaled parameters of the EOS I. On the basis of Eqs. (8a) and (8b), a is predicted to be linear in $1/T$, and also b to be proportion to the reciprocal of temperature. Here, by using the values of the given parameters in Table 1, we evaluated such predictions for Ar, Kr and Xe to investigate the temperature dependencies of the scaled parameters, a and b. In Fig. 2a and b, the temperature dependencies of the scaling parameters of Ar, Kr and Xe have been shown. These figures show perfect linearity in the whole temperature range that experimental data are reported. Also such results show that the parameter a_2 is independent of temperature and density in the range of given experimental data. As shown in Fig. 2b, each line has no intercept unlike Fig. 2a which is expected. The values of a_2 for Xe, Kr and Ar are found to be 0.012403, 0.0069331 and 0.0039472 ($L^2\,mol^{-2}$), respectively.

3. Deriving linear isotherm for the ionic and metallic solids

3.1. Theoretical aspects

In some fluids and solids, the species interact very much with an appreciable coulombic feature with each other that the long-range dispersive interaction potential is underestimated if it is treated by only a simple sixth power of inverse of interatomic distance. Also, the repulsive side of this potential for these kinds of fluids and solids has been analyzed in terms of an inverse power law [22,23], and it is found that the interionic dipole–dipole interaction has an effect on softening the repulsive part of the pair potential [24,25]. From the forgoing analysis of the experimental data and from the fact that the range of fluid densities correspond to the interatomic distances mainly located around the potential minimum (r_m) and likely is extended to larger atomic distance than r_m, Ghatee and Bahadori supposed LJ (6, 3) for compressed liquid alkali metals, especially for compressed liquid cesium [26].

From the discussion mentioned above, we propose that the potential function as binding energy comes from LJ (6, 3) for the metallic and ionic solids.

In the case of LJ (6, 3) for ionic and metallic solids, the final form of the new EOS can be derived which is the same as the Ghatee and Bahadori EOS, according to which $(Z-1)\upsilon^2$ is linear with respect to $1/\rho$ for each isotherm of a solid (hereafter referred to as EOS II),

$$(Z-1)\upsilon^2 = c + d\left(\frac{1}{\rho}\right) \tag{10}$$

where Z and $\rho = 1/\upsilon$ have the same meaning as in EOS I, and c and d are temperature-dependent parameters, as follows:

$$c = c_2 + \frac{c_1}{T} \tag{11a}$$

and

$$d = \frac{d_1}{T} \tag{11b}$$

where d_1 and c_1 are related to the attraction and repulsion terms of the average effective pair potential, respectively, while c_2 like a_2 in Eq. (9) is related to the vibrational energy effects. Again, we may expect that c_2 becomes almost a constant, like a_2.

3.2. Experimental test of EOS II for metallic and ionic solids

To consider how EOS II works for the metallic, ionic, and also non-ionic and non-metallic solids, we select the same solids as in Fig. 1 and the accuracy of EOS II is investigated diagrammatically in Fig. 3a–c. As may be seen in these figures, EOS II is suitable for Au and NaCl, but not for Ar. The results of such a fitting of the experimental data for Au [27], Ag [27], Cu [28,29], NaF [30], LiF [30], CsCl [30], NaCl [31] and MgO [31] into EOS II, are summarized in Table 2. As one may see from the correlation coefficients, the EOS II presented in this study works quite well for the ionic and metallic solids over the whole range of pressure and temperature for which the experimental data are reported.

3.3. Temperature dependencies of the parameters of EOS II

Just like Eqs. (8a) and (8b), one may consider Eqs. (11a) and (11b), as temperature dependencies of the parameters of EOS II; to be specific, it is expected that d be proportional to $1/T$ and c varies linearly with respect to $1/T$. Taking the values of the scaling parameters from Table 2, our expectation for Au, NaF and LiF are illustrated in Fig. 4a and b. As can be seen from Fig. 4a and b, c and d are linear in $1/T$ as expected from Eqs. (11a) and (11b). In addition, these results may suggest that the parameter c_2 is independent of

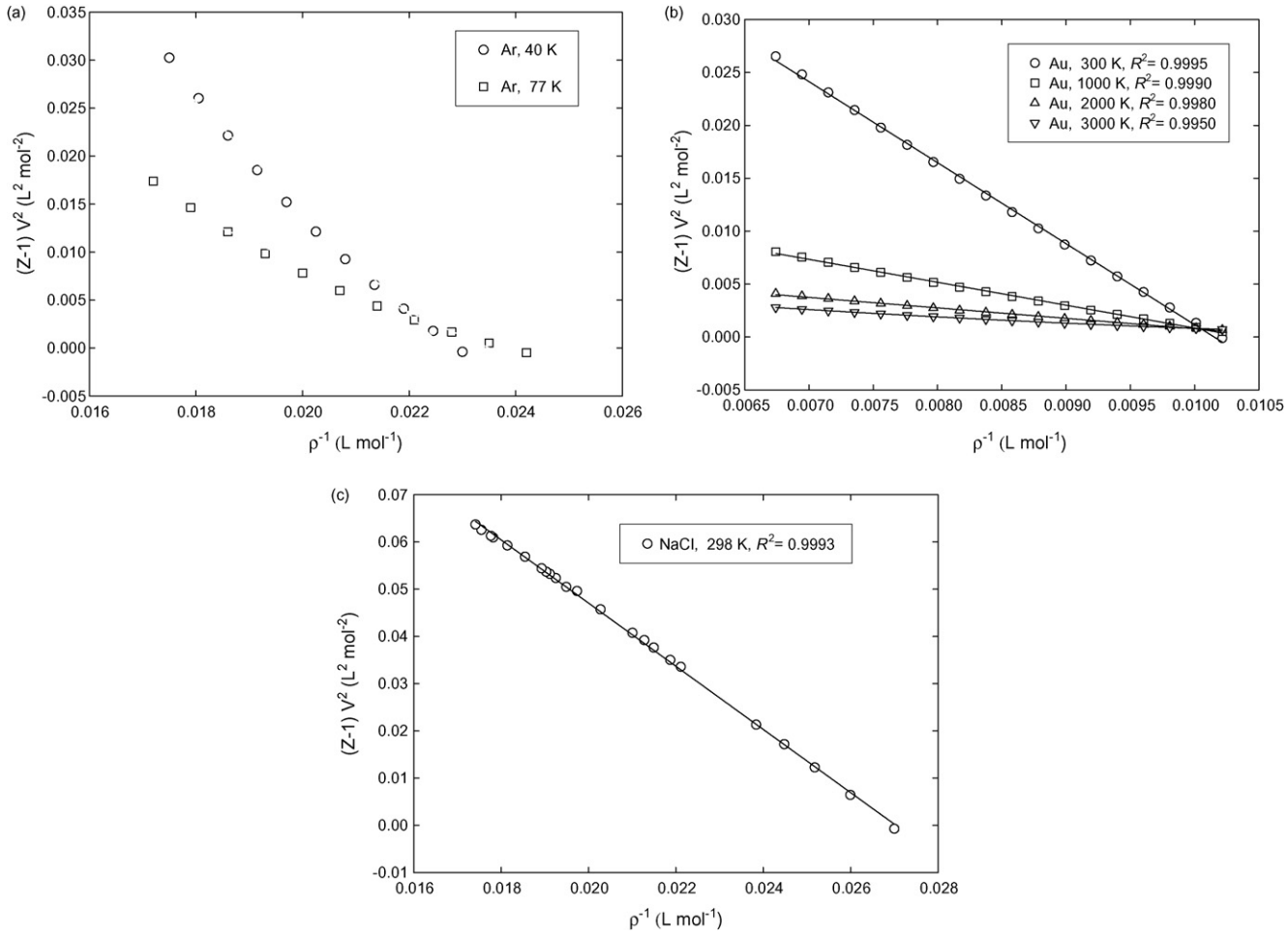

Fig. 3. Fitting experimental data of given isotherm(s) into EOS II for (a) Ar, (b) Au, (c) NaCl. Note the significant nonlinearity of the first case.

temperature and density in the range of given experimental data. The values of c_2 for Au, NaF and LiF are respectively −0.0018177, −0.0010710 and −0.00072837 ($L^2\,mol^{-2}$) by the best fitting curve shown in Fig. 4a.

4. Temperature and density dependence of physical properties

On the basis of the EOSs proposed, we show that the temperature dependencies of the internal energy is separable from its density dependencies. Hence, the heat capacity of a solid is independent of its density, interaction potential parameters and also non-ideal thermal pressure. Nevertheless, unlike the heat capacity, the isothermal compressibility and the isobaric thermal expansivity both depend on all of them.

We may substitute $Z = pv/kT$ into either EOS I or EOS II and solve for the pressure to obtain,

$$\frac{p}{kT} = \frac{I}{v} + \frac{J(T)}{v^{n'}} + \frac{K(T)}{v^{m'}} \tag{12}$$

where n' and m' are positive integers and

$$J(T) = J_0 + \frac{J_1}{T} \tag{13a}$$

$$K(T) = K_0 + \frac{K_1}{T} \tag{13b}$$

where I, J_0, J_1, K_0 and K_1 are constants.

We may then use Eq. (12) and $(\partial \ln Q/\partial v)_T = p/kT$ to derive an expression for the canonical partition function:

$$\ln Q = I \ln v + \frac{J(T)}{(1-n')v^{n'-1}} + \frac{K(T)}{(1-m')v^{m'-1}} + f(T) \tag{14}$$

where $f(T)$ is a function of temperature.

Eq. (14) may be used to obtain an expression for the internal energy:

$$E = k\left[\frac{J_1}{(n'-1)v^{n'-1}} + \frac{K_1}{(m'-1)v^{m'-1}} + T^2 f'(T)\right] \tag{15}$$

where

$$f'(T) = \frac{\mathrm{d}f(T)}{\mathrm{d}T}$$

Note that the first two terms of Eq. (15) is E_0 and the last term is E_{vib} of Eq. (4). Hence for the heat capacity at constant volume, C_V, we obtain,

$$C_V = k[T^2 f''(T) + 2Tf'(T)] \tag{16}$$

We do not know the functional form of $f(T)$, but expect to depend on the type of solid. For instance, it is a cubic function for a molecular solid when $T \to 0$ due to the well known T^3-law:

$$C_V = a_0 T^3 \ \text{ as } \ T \to 0 \tag{17}$$

Hence, we may expect that the proportionality constant a is independent of density, the interaction potential parameters and

Table 2
The parameters of EOS II (c and d), coefficient of determination (R^2), range of pressure data (Δp) and calculated percent density deviation $(\Delta\rho/\rho)\times 100$ for different ionic and metallic solids at given temperatures

Solid	T (K)	c ($\times 10^3$ L^2 mol^{-2})	d ($\times 10$ L^3 mol^{-3})	R^2	Δp (kbar)	100 ($\lvert\Delta\rho\rvert/\rho$)[a]
[b]Au	300	77.725	−76.560	0.9995	0–2160	0.21 (0.49)
	500	46.161	−45.181	0.9993	14–2170	0.23 (0.55)
	1000	22.490	−21.644	0.9990	50–2190	0.28 (0.69)
	1500	14.598	−13.796	0.9989	86–2220	0.33 (0.84)
	2000	10.656	−9.8755	0.9980	122–2250	0.39 (0.98)
	2500	8.2864	−7.5187	0.9970	158–2270	0.45 (1.28)
	3000	6.7086	−5.9496	0.9950	194–2300	0.51 (1.28)
[c]NaF	298	61.660	−40.968	1.0000	0–90	0.02 (0.03)
	473	37.978	−24.804	0.9995	0–90	0.06 (0.12)
	673	26.940	−17.261	0.9998	0–90	0.04 (0.08)
	873	20.679	−12.972	1.0000	0–90	0.01 (0.04)
	1073	15.977	−9.7581	0.9995	0–90	0.06 (0.14)
[c]LiF	298	23.263	−23.830	0.9994	0–90	0.16 (0.34)
	573	11.785	−11.728	0.9988	0–90	0.09 (0.17)
	873	7.6426	−7.3112	0.9992	0–90	0.07 (0.16)
	1073	5.7674	−5.3343	0.9985	0–90	0.12 (0.24)
[c]CsCl	298	562.17	−133.65	1.0000	0–90	0.02 (0.06)
	473	327.88	−76.080	1.0000	0–90	0.03 (0.06)
	673	213.99	−48.072	1.0000	0–90	0.01 (0.051)
	873	151.15	−32.778	1.0000	0–90	0.04 (0.09)
[d]NaCl	298	180.89	−66.911	0.9993	0–300	0.199 (0.54)
[e]Cu	298	19.725	−27.821	1.0000	60–1000	0.03 (0.09)
[f]Cu	298	20.234	−28.653	0.9991	60–7200	0.29 (0.68)
[e]Ag	298	50.744	−49.839	0.9997	75–1000	0.114 (0.27)
[g]Pb	298	99.997	−55.843	0.9988	900–10000	0.197 (0.33)
[e]Pd	298	54.752	−61.760	1.0000	65–800	0.05 (0.06)
[e]Mo	298	76.478	−80.964	0.9991	75–1000	0.157 (0.32)
[d]Nb	298	76.853	−70.832	0.9988	0–500	0.16 (0.30)
[d]MgO	298	39.796	−46.973	0.9990	0–400	0.116 (0.27)

[a] The maximum percent deviation is given in the parentheses.
[b] Ref. [27].
[c] Ref. [30].
[d] Ref. [31].
[e] Ref. [28].
[f] The experimental data are taken from Refs. [28,29] reported by Nellis et al.
[g] Ref. [29].

non-ideal thermal pressure. However, for a metallic lattice at very low temperature,

$$C_V = a_0 T^3 + b_0 T \tag{18}$$

where the second term is the contribution of valance electrons in C_V.

Making use of Eq. (12), one may derive the isothermal compressibility, k_T, and isobaric thermal expansivity, α,

$$\kappa_T = \frac{\left[\frac{I}{\nu} + \frac{n'J(T)}{\nu^{n'}} + \frac{m'K(T)}{\nu^{m'}}\right]^{-1}}{kT} \tag{19}$$

$$\alpha = \left[\frac{I}{\nu} + \frac{J_0}{T\nu^{n'}} + \frac{K_0}{T\nu^{m'}}\right]\left[\frac{I}{\nu} + \frac{n'J(T)}{\nu^{n'}} + \frac{m'K(T)}{\nu^{m'}}\right]^{-1} \tag{20}$$

Based on Eqs. (19) and (20), α and k_T depend on T, v and the potential parameters.

5. Comparison with other EOSs

It is ordinary to express the EOS in solids in terms of the zero-pressure density, ρ_0, bulk modulus at zero pressure limit, B_0, and also its first pressure derivative, B_0'. Therefore, we may express the parameters of EOSs I and II in terms of ρ_0 and B_0. The final results for EOS I is,

$$a = \frac{-1}{\rho_0^2}\left(2 + \frac{B_0}{2\rho_0 RT}\right), \qquad b = \frac{1}{\rho_0^4}\left(\frac{B_0}{2\rho_0 RT} + 1\right) \tag{21a}$$

and for EOS II,

$$c = \frac{1}{\rho_0^2}\left(1 + \frac{B_0}{\rho_0 RT}\right), \qquad d = \frac{-1}{\rho_0}\left(\frac{B_0}{\rho_0 RT} + 2\right) \tag{21b}$$

Eqs. (21a) and (21b) show that the new EOSs have two parameters which may be given only in terms of ρ_0 and B_0. The values of ρ_0 in Eqs. (21a) and (21b) are obtained by setting the pressure in Eqs. (7) and (10) equal to 0. Once obtaining the values of ρ_0 at a given temperature one can calculate the value of B_0 at that temperature. Finally, the values of B_0' may be obtained from Eqs. (7) and (10), respectively, of course by using the definition of B_0',

$$B_0' = \left(\frac{\partial B}{\partial p}\right)_{p=0} = \frac{1 + 9a\rho_0^2 + 25b\rho_0^4}{1 + 3a\rho_0^2 + 5b\rho_0^4} \tag{22a}$$

$$B_0' = \left(\frac{\partial B}{\partial p}\right)_{p=0} = \frac{1 + 9c\rho_0^2 + 4d\rho_0}{1 + 3c\rho_0^2 + 2d\rho_0} \tag{22b}$$

To investigate the accuracy of the new EOSs, we have compared the calculated values of ρ_0, B_0 and B_0' from EOS I for argon and xenon with the experimental values [18] in Table 3, and also the values of B_0 and B_0' for some solids with those obtained from other EOSs in Table 4, namely, Jiuxun et al. (SJX) [32], Sushil-Papiya (SP) [33], Huang-Chow (HC) [34], Parsafar–Mason (PM) [2], Vinet et al. [1], Freund-Ingalls (FI) [35], Effective Rydberg (ER2) [36], Hozapfel (Hzp) [37], Kumari-Dass (KD) [38] and Modified Generalized Lennard–Jones (mGLJ) [39]. The value of B_0' obtained

Table 3
Comparison of the calculated values of ρ_0, B_0 and B'_0 from EOS I with experimental values for argon and xenon

Solid	T (K)	v_0 (exp) (cm^3/mol)	v_0 (cal) (cm^3/mol)	B_0 (exp) (kbar)	B_0 (cal) (kbar)	B'_0 (exp)	B'_0 (cal)
Ar	4	22.557	22.638	28.6	26.2	7.2	8.00
	20	22.645	22.723	27.6	25.2	7.3	8.02
	40	23.026	23.085	23.5	22.3	7.5	8.05
	60	23.611	23.600	18.6	19.1	7.8	8.08
	77	24.290	24.170	14.1	16.2	8.4	8.13
Xe	20	34.823	34.926	35.6	34.8	7.3	7.7
	60	35.558	35.625	30.2	29.8	7.5	7.8
	100	36.545	36.538	24.6	24.5	7.6	8.0
	120	37.090	37.025	22.5	22.4	7.6	8.0
	159	38.500	38.275	14.8	15.6	8.8	8.8

by EOS II is in better agreement with experimental value than that of the EOS I. Owing to the fact that B'_0 strictly depends on the exponent of the binding energy in Eq. (3), one may conclude that exponent (12, 6) is slightly larger than the actual value.

In addition, the average percent error of pressure for some solids has also been compared with those obtained from some other EOSs in Table 5; Effective Rydberg (ER2) EOS [36], Hozapfel (Hzp) EOS [37], Kumari-Dass (KD) EOS [38], Baonza EOS [40], Marnaghan type EOS proposed by Jiuxun [41] (SMnh), Vinet EOS [1], and Modified Generalized Lennard–Jones (mGLJ) EOS [39]. As can be seen, the predictions of EOS II are comparable with other ones, even with its simplicity.

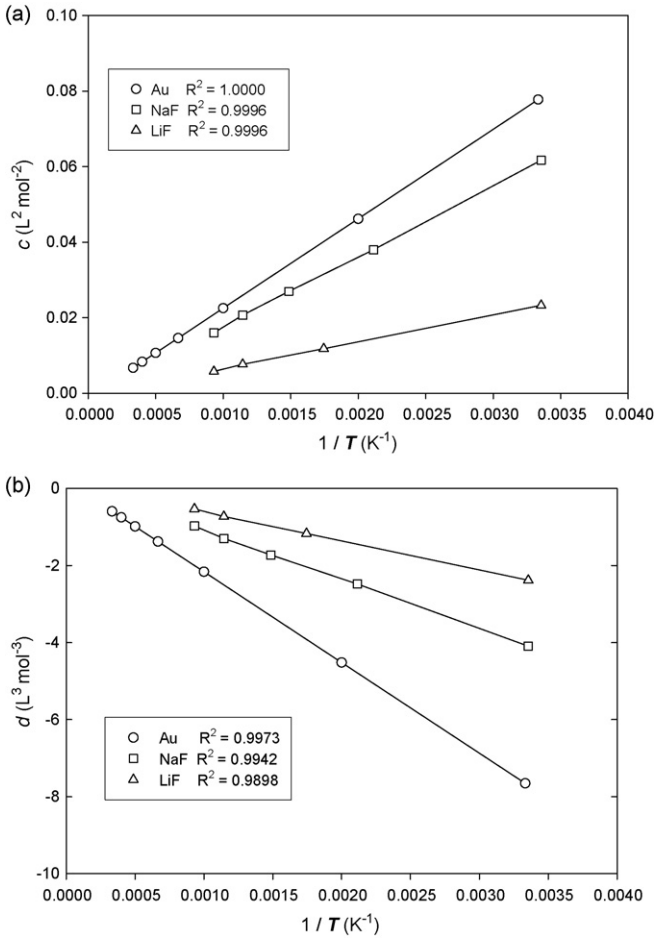

Fig. 4. Temperature dependence of (a) the intercept c and (b) slope d parameters, for Au, NaF and LiF in which all are well fitted onto Eqs. (11a) and (11b).

Table 4
Experimental values of B_0 and B'_0 for some solids compared with those calculated by using different EOSs, for given temperatures

Solids	EOSs	B_0 (kbar)	B'_0
n-H_2 (T = 4.2 K)	ER2	1.5185	7.690
	Hzp	1.3975	8.371
	KD	1.786	6.998
	SJX	1.706	7.036
	PM	2.10	5.85
	SP	1.7	6.78
	This study	1.614	8.073
	Experimental value	1.70 (±0.006)	7.0 (±0.3)
n-D_2 (T = 4.2 K)	KD	3.46	5.32
	SP	3.16	6.51
	PM	3.69	5.75
	This study	3.10	8.04
	Experimental value	3.15 (±0.06)	6.7 (±0.3)
Au (T = 300 K)	KD	1850	4.839
	Hzp	1848.9	5.005
	SJX	1845.9	5.024
	mGLJ	1848.2	4.9877
	This study	1841.8	5.003
Cu (T = 298 K)	KD	1431.93	4.339
	SP	1389	4.92
	mGLJ	1416.0	4.652
	This study	1356.3	5.005
NaCl (T = 298 K)	HC	239.98	4.721
	FI	239.19	4.745
	KD	240.14	4.54
	SP	236.8	4.90
	PM	241	4.90
	mGLJ	238.36	4.766
	Vinet	235.0	5.35
	This study	223.01	5.01
	Experimental value	235.6	5.11 (±0.03)

6. Investigation of some regularities using the linear isotherms

The EOSs I and II may be used to derive the common compression point, ρ_{oz}, as well as the common bulk modulus point, ρ_{OB}, for solids as LIR EOS was applied to dense fluids. By setting the partial derivative of Z or $(Z-1)\upsilon^2$ with respect to temperature equal to zero

Table 5
The average percent error of pressure of EOS II for some solids, compared to those calculated from other EOSs at 298 K

Solids	ER2	Hzp	KD	SMnh	Vinet	Baonza	mGLJ	This study
Cu	0.83	0.743	0.90	0.664	1.05	0.676	0.603	0.66
Ag	1.15	0.66	0.79	0.503	0.821	0.617	0.409	0.99
Au	0.94	0.89	0.98	0.95	0.938	0.957	0.65	1.11
LiF	0.48	0.482	0.45	0.35	0.571	0.38	0.337	0.60
NaF	0.60	0.58	0.61	0.57	0.604	0.57	0.501	0.31
Mo	1.47	1.51	1.44	1.22	1.468	1.507	1.039	1.50

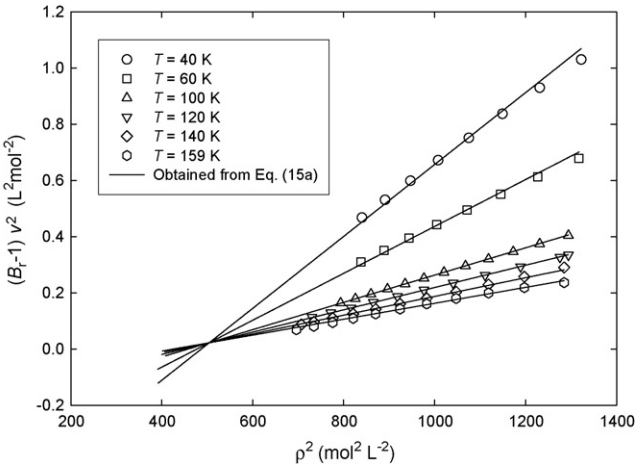

Fig. 5. Search for the linearity of $(B_r - 1)\upsilon^2$ vs. ρ^2 for some isotherms of Xe; points are obtained from experimental data [18], and all lines from Eq. (24a) and fitting data.

at $\rho = \rho_{oz}$, we may obtain ρ_{oz} for EOSs I and II, respectively as,

$$\rho_{oz} = \left(-\frac{a_1}{b_1}\right)^{0.5} \tag{23a}$$

$$\rho_{oz} = \left(-\frac{d_1}{c_1}\right) \tag{23b}$$

As shown in Fig. 1a for argon and Fig. 3b for Au, all isotherms pass through a common point which is the common compression point. The calculated value of ρ_{oz} for Xe given by Eq. (23a) is 28.35 mol L^{-1} which is comparable with experimental value obtained from isotherms, 28.94 mol L^{-1} in the range of 20–60 K. Moreover, the calculated value of ρ_{oz} for Au obtained from Eq. (23b) is 95.6 mol L^{-1} which has only a small deviation from the experimental value obtained from the intersection point of isotherms lower than 1000 K of Fig. 3b (≈99.10 mol L^{-1}).

Using EOS I, the reduced bulk modulus, $B_r = B/\rho RT$ $[B = -\upsilon(\partial p/\partial \upsilon)T]$, is obtained as

$$(B_r - 1)\upsilon^2 = 3a + 5b\rho^2 \tag{24a}$$

and from EOS II,

$$(B_r - 1)\upsilon^2 = 3c + 2d\left(\frac{1}{\rho}\right) \tag{24b}$$

In order to find the common bulk modulus point, ρ_{OB}, one may set $(\partial B_r/\partial T)_\rho$ equal to zero, for EOSs I and II, to obtain the following results;

$$\rho_{OB}^2 = -0.6\frac{a_1}{b_1}(\text{from EOS I}) \quad \text{and} \quad \rho_{OB} = -\frac{2}{3}\frac{d_1}{c_1}(\text{from EOS II}) \tag{25}$$

The accuracy of Eq. (24a) for some isotherms of xenon is shown in Fig. 5. Even though the isotherms do not intersect in the solid density range, their extrapolations give a common point at a lower density. The calculated value of ρ_{OB} for Xe using Eq. (25) is about 22.34 mol L^{-1} which is below ρ_0 of the isotherms.

7. Discussions and conclusions

LIR, which was derived on the basis of the concept of the effective pair potential, has been applied well to most Lennard–Jones fluids which their interaction potential can be modeled rather accurately by the (12-6) powers of inverse intermolecular distance. This is because the nature of forces of Lennard–Jones fluids is well described according to a definite dispersive interaction mechanism. However, the application of LIR to quite non-spherical molecules such as long chain organic compounds [42], alkali metals liquids such as liquid cesium [26] and some complex mixtures [6] in which the LJ (12-6) potential function is not appropriate, isotherms may, significantly, deviate from the linear behavior. In different studies in solids, Vinet et al. [1] derived a universal EOS for solids on the basis of a universal relation for the binding energy of solids in terms of intermolecular distances. Parsafar and Mason [2] later derived another appropriate EOS for compressed solids using the fact that the repulsive branch of the binding energy curves can be well given by a simple cubic function of density. In this study, LIR EOS in which $(Z-1)\upsilon^2$ is linear with respect to ρ^2 has been tested for some ionic, metallic and molecular (non-ionic and non-metallic) solids, and observed that it is suitable only for the last one, see Fig. 1a; nevertheless, for the ionic and metallic solids due to their ionic characteristic for which the repulsive part of their potential is softer than that of LJ (12, 6) and the attractive part has a longer range than that of LJ (12, 6), the linearity of $(Z-1)\upsilon^2$ exists in terms of $1/\rho$ rather than ρ^2, see Figs. 1b, c, and 2b, c. Therefore, we may conclude that EOS is sensitive to the functional form of the interaction or binding energies.

In general, as long as the non-ideal thermal pressure is constant or varies very slowly with temperature and density, all dense systems mimic the same *pVT* behavior and the form of EOS is not influenced by the physical state of material, but the physical state only affects the scaling parameters. For instance, Marnaghan EOS [43] based on the empirical observation in which the isothermal bulk modulus is a linear function of pressure has been wildly used for both solids and liquids. In harmony, it was found that it is also applicable to dense supercritical fluids [9]. In this study, we have also shown that a condense matter obeys from the same mathematical expression for its EOS regardless of its physical state. However, the values of its parameters depend on the physical state. Due to the fact the binding energy depends on the average molecular separation and the physical state of matter such a conclusion is expected. Additionally, such dependencies show that the isobaric expansivity and isothermal compressibility are density and state dependent, see Eqs. (19) and (20). In solids, the vibrational contribution in EOS like the non-ideal thermal pressure in fluids may be temperature and density dependent with a complicated form [3,17]; nonetheless, its constancy leads to a reasonable result for solids. By using this approximation, EOSs I and II may, accurately, show the behavior of *pVT* in solids. We have also noticed that both EOSs mimic the simple form of temperature dependencies which are shown in Figs. 2a, b and 4a and b for the molecular and non-molecular solids, respectively.

As mentioned before, the parameters a_0 and b_0 in Eqs. (17) and (18) are expected to be independent of lattice density and the interaction potential. Owing to the fact that such a contribution is due to the long wavelength vibrational modes, in which the atomic nature of solid becomes unimportant; in other words, the solid may be assumed to be an elastic medium; such a conclusion is reasonable.

By careful inspection of Tables 3–5, one may come to this fact that the new two-parameter EOSs are comparable with other two-parameter and three-parameter EOSs presented in literature. However, the advantages of these new EOSs over the previous ones are (1) they have very simple temperature-dependent parameters; (2) the parameters have physical meaning; and finally, (3) they can, at least, predict two solid regularities, which are in accordance with experiment.

References

[1] P. Vinet, J. Ferrante, J.R. Smith, J.H. Rose, J. Phys. C 19 (1986) L467;
P. Vinet, J.R. Smith, J. Ferrante, J.H. Rose, Phys. Rev. B 35 (1987) 1945.
[2] G.A. Parsafar, E.A. Mason, Phys. Rev. B 49 (1994) 3049.
[3] G.A. Parsafar, E.A. Mason, J. Phys. Chem. 97 (1993) 9048.

[4] E. Keshavarzi, G.A. Parsafar, J. Phys. Chem. B 103 (1999) 6584.
[5] M.H. Ghatee, M. Bahadori, J. Phys. Chem. B 108 (2004) 4141.
[6] G.A. Parsafar, E.A. Mason, J. Phys. Chem. 98 (1994) 1962.
[7] G.A. Parsafar, N. Sohrabi, J. Phys. Chem. 100 (1996) 12644.
[8] B. Najafi, G.A. Parsafar, S. Alavi, J. Phys. Chem. 99 (1995) 9248.
[9] S. Alavi, G.A. Parsafar, B. Najafi, Int. J. Thermophys. 16 (1995) 1421.
[10] V. Moieni, J. Phys. Chem. B 110 (2006) 3271.
[11] J. Tian, Y. Gui, J. Phys. Chem. B 111 (2007) 1721.
[12] M. Pickholz, Z. Gamba, Phys. Rev. B 53 (1996) 2159.
[13] T. Sun, A.S. Teja, J. Phys. Chem. 100 (1996) 17365.
[14] G.A. Parsafar, F. Kermanpour, B. Najafi, J. Phys. Chem. B 103 (1999) 7287.
[15] M. Ross, D.A. Young, Annu. Rev. Phys. Chem. 44 (1993) 61.
[16] L.A. Girifalco, Statistical Mechanics of Solids, Oxford University Express, New York, 2000 (Chapter 5).
[17] M. Shokouhi, G.A. Parsafar, Fluid Phase Equilibria 264 (2008) 1.
[18] M.S. Anderson, C.A. Swenson, J. Phys. Chem. Solids 36 (1975) 145.
[19] J.W. Stewart, J. Phys. Chem. Solids 1 (1956) 146.
[20] M.S. Anderson, C.A. Swenson, Phys. Rev. B 10 (1974) 5184.
[21] O. Olabisi, R. Simha, Macromolecules 8 (1975) 206;
S. Saeki, F. Wang, Y. Tanaka, Polymer 47 (2006) 7455.
[22] S. Munejiri, F. Shimojo, K. Hoshino, M. Watabe, J. Phys.: Condens. Matter 9 (1997) 3303.
[23] N. Matsuda, K. Hoshino, M. Watabe, J. Chem. Phys. 93 (1990) 7350.
[24] K.K. Mon, N.W. Ashcroft, G.V. Chester, Phys. Rev. B 19 (1979) 5103.
[25] J.J. Rehr, E. Zaremba, W. Khon, Phys. Rev. B 12 (1975) 2062.
[26] M.H. Ghatee, M. Bahadori, J. Phys. Chem. B 105 (2001) 11256.
[27] D.L. Heinz, R. Jeanloz, J. Appl. Phys. 55 (4) (1984) 885.
[28] H.K. Mao, P.M. Bell, J.W. Shaner, D.J. Steinberg, J. Appl. Phys. 49 (1978) 3276.
[29] W.J. Nellis, J.A. Moriarty, A.C. Mitchell, M. Ross, R.G. Dandrea, Phys. Rev. Lett. 60 (14) (1988) 1414.
[30] T. Yagi, J. Phys. Chem. Solids 39 (1978) 561.
[31] E.A. Perez-Albuerne, H.G. Drickamer, J. Chem. Phys. 43 (4) (1965) 1381.
[32] S. Jiuxun, W. Qiang, C. Lingcang, J. Fuqian, Physica B 371 (2006) 257.
[33] S.B. Roy, P.B. Roy, J. Phys.: Condens. Matter 11 (1999) 10375.
[34] Y.K. Huang, C.Y. Chow, J. Phys. D: Appl. Phys. 7 (1974) 2021.
[35] J. Freund, R. Ingalls, J. Phys. Chem. Solids 51 (1989) 263.
[36] F.D. Staccy, B.J. Brennan, R.D. Irrvine, Geophys. Surv. 4 (1981) 189.
[37] W.B. Holzapfel, Phys. Rev. B 67 (2003) 026102;
W.B. Holzapfel, J. Phys.: Condens. Matter 14 (2002) 10525;
W.B. Holzapfel, High Pressure Res. 22 (2002) 209.
[38] M. Kumari, N. Dass, J. Phys: Condens. Matter 2 (1990) 3219;
M. Kumari, N. Dass, J. Phys: Condens. Matter 2 (1990) 7891.
[39] J.O. Hirschfelder, C.F. Curtiss, R.B. Bird, Molecular Theory of Gas and Liquids, John Wiley & Sons, 1964.
[40] V.G. Baonza, M. Caceres, J. Nunez, Chem. Phys. Lett. 216 (1993) 579;
V.G. Baonza, M. Caceres, J. Nunez, Chem. Phys. Lett. 228 (1994) 137;
V.G. Baonza, M. Caceres, J. Nunez, J. Phys. Chem. 98 (1994) 4955.
[41] S. Jiuxun, J. Phys.: Condens. Matter 17 (2005) L103.
[42] G.A. Parsafar, Z. Kalantar, Fluid Phase Equilibr. 234 (2005) 11.
[43] F.D. Marnaghan, Proc. Natl. Acad. Sci. U.S.A. 30 (1944) 244.

Mohammad Shokouhi
Gholam Abbas Parsafar*
Mohammadhasan Dinpajooh
Department of Chemistry, Sharif University of Technology, Azadi Avenue, Tehran 1458881367, Iran

* Corresponding author. Tel.: +98 21 66165355;
fax: +98 21 66005718.
E-mail addresses: shokouhi110@gmail.com (M. Shokouhi), parsafar@sharif.edu (G.A. Parsafar), dinpa001@umn.edu (M. Dinpajooh)

5 June 2008
Available online 26 July 2008